Electronic Supplementary Material (ESI) for Journal of Materials Chemistry B.

Optimized silicate nanozymes with atomically incorporated iron and manganese for intratumoral coordination-enhanced once-for-all catalytic Therapy

Xiuping Xu[a,d], Shuang Liu[a], Jin Ye[a], Qiang Wang[a], Mengting Liu[a], Yunlong Li[a], Hang Shangguan[a], Kefen Zhang[*d], Yujie Fu[c], and Jiating Xu[*a,b]

[a] Key Laboratory of Forest Plant Ecology, Ministry of Education, College of Chemistry, Chemical Engineering and Resource Utilization, Northeast Forestry University, Harbin 150040, P. R. China

[b] Heilongjiang Provincial Key Laboratory of Ecological Utilization of Forestry-Based Active Substances, Northeast Forestry University, Harbin, 150040, P. R. China

[c] College of Biological Sciences and Technology, Beijing Forestry University, Beijing 100083, P.R. China

[d] Guangxi University of Science and Technology, Liuzhou 545006, China

Materials

Triethanolamine (TEOA), Hexadecyltrimethylammonium p-toluenesulfonate (CTA·Tos), 1-butyl-3-methylimidazolium trifluoromethanesulfonate ([BMIM] OTF), ammonium chloride (NH_4Cl), urea (CH_4N_2O), methoxy-polyethylene glycol (mPEG), 5,5-dimethyl-1pyrroline N-oxide (DMPO), 3-(4, 5-dimethyl-2-thiazolyl)-2,5-diphenyl-2-H-tetrazolium bromide (MTT), fluorescein isothiocyanate (FITC), 1,1′,3,3′-tetraethyl-imidacarbocyanine (JC-1) and 4′,6-diamidino-2-phenylindole (DAPI) were obtained from the Aladdin Reagents Company Co., Ltd. Tetraethoxysilicon (TEOS), ammonium chloride (NH_4Cl), gallate (GA), methylene blue (MB) and 1,4-benzoquinone (BQ) were purchased from RHAWN Chemical Agents. Ferric acetylacetonate ($Fe(acac)_3$) was gained from Shanghai DiBo Biochemical Co., Ltd. Manganese (II) chloride tetrahydrate ($MnCl_2·4H_2O$), Phosphate buffer solution (PBS) (pH 7.4), Phosphate buffer solution (PBS) (pH 6.5) and fetal bovine serum (FBS) were purchased from Beyotime Biotechnology Co., Ltd., and ethanol (C_2H_5OH) were got from Tianjin Institute of Chemical Agents. Dulbecco's Modified Eagle Medium (DMEM) was received from HyClone. 1,3-Diphenylisobenzofuran (DPBF), glutathione (GSH), 5,5-dithiobis (2-nitrobenzoic acid) (DTNB), 2′,7′-dichlorodihydrofluorescein diacetate (DCFH-DA), hydrogen peroxide (H_2O_2), calcein AM and propidium iodide (PI) were ordered from Beijing Solarbio Science & Technology Co., Ltd. All of the chemical reagents were used without further purification.

Characterization

The morphology of the sample was analyzed by scanning electron microscope (SEM, JSM-6700F) and transmission electron microscope (JEM-2100) (Japan electronics). X -ray powder diffractometer (Shimadu RD-7000) was employed to investigate the crystallographic

properties of the catalyst. Energy disperse X-ray (EDX) was performed on a field emission scanning electron microscope (JSM-7610F) to analyze elemental features of the samples. The chemical composition and element valence were analyzed using X-ray photoelectron spectroscopy (XPS, Kratos Axis Ultra) with a monochromated Al Kα X-ray source (hν=1486.6 eV). DLS measurements were performed using a Malvern Nano-zetasizer. N_2 adsorption-desorption isotherm measurements were investigated to study the Brunauer-Emmett-Teller (BET) specific surface areas of the samples. Fe K-edge and Ca K-edge EXAFS and XANES spectra were performed with Si (111) crystal monochromators at the BL11B beamlines at the Shanghai Synchrotron Radiation Facility (SSRF) (Shanghai, China). The electron spin resonance (ESR) spectra were examined on a Bruker ELEXSYS-II E500 CW-EPR. The infrared spectra were measured using a Fourier-transform infrared spectrometer Spectrum 400 (PerkinElmer) within the range of wavenumbers 4000-550 cm^{-1}. The ultraviolet-visible-infra-red (UV-vis-NIR) spectrometry was measured on UH5700 spectrophotometer. Time-resolved photoluminescence (TRPL) spectra for samples were conducted from 350 to 600 nm with a photoluminescence spectrometer (QM8000) at an excitation 325 nm. Electrochemical characterizations were performed on an electrochemical workstation (CHI660E) using a three-electrode system (pH 7.0) with Pt as the counter electrode, Ag/AgCl as the reference electrode, and ITO as the working electrode under visible light. Photoluminescence (PL) spectroscopy was recorded *via* an Agilent Cary Eclipse (F-7000) at room temperature. Elemental analyses were conducted on inductively coupled plasma-optical emission spectrometry (ICP-OES) (Agilent 5110). The cell fluorescence imaging experiments were carried out using confocal laser scanning fluorescence microscope (CLSM). Cell viabilities were measured by recording

the absorption at 490 nm by using a Microplate Reader. The flow cytometry data was obtained by CytoFLEX S.

Synthesis of mesoporous silica nanoparticles (MSNs)

Monodispersed MSNs with the diameter of 110 nm were synthesized according to previous reports. Briefly, CTA·Tos (0.96 g), TEA (0.105 g), and [BMIM] OTF (10 mg) were first mixed in 50 mL of water, then the mixture was stirred at 80 °C for 1 h. Next, 7.8 mL of TEOS was quickly added into the mixture. After stirring at 80°C for another 2 h, the mixture was purified by washing and centrifugation with ethanol and water. Then, template extraction was employed to remove the CTA·Tos from as-prepared MSNs. After addition of ethanolic HCl (concentrated HCl (15 mL) in ethanol (100 mL) into 0.1 g of the as-prepared MSNs, the suspension was sonicated for 2 h and then stirred at 70 °C for 24 h. This e5xtraction procedure was repeated three times. Finally, the precipitate was collected by washing with ethanol and drying in a vacuum oven at 60 °C for 24 h.

Synthesis of mesoporous iron and manganese silicate nanospheres (designated as FMMSNs)

FMMSNs were synthesized by hydrothermal treatment, and the MSNs were used as self-sacrificing templates. Briefly, $Fe(acac)_3$ (0.25 mmol), urea 1.35 g, and NH_4Cl (10 mmol) were first mixed in 20 mL water, The obtained mixture of coordination complex ions was solution A. MSNs (50 mg) and $MnCl_2 \cdot 4H_2O$ (0.125 mmol) were mixed in 20 mL water to obtain solution B. Solutions A and B were mixed and stirred for 30 min, then transferred into a Teflon-lined autoclave (50 mL) and maintained at 200 °C for 12 h. After cooling down to room temperature, the obtained product was rinsed with water and ethanol three times, respectively.

Synthesis of PEGylated FMMSNs (designated as FMMP)

FMMSNs (100 mg) and methoxy PEG silane (50 mg) were homogenized in ethanol (50 mL), followed by heating at 60 °C to allow the reaction for 24 h. After cooling down to room temperature, the obtained product was rinsed with water and ethanol three times, respectively.

Histological examination

Two weeks of therapy later, the main organs (heart, liver, spleen, lung, kidney) and tumors were collected from groups 1-6. Next, the H&E assay was used to confirm whether FMMPG could cause injury to the organs or not. At the same time, H&E assays of tumors collected from groups 1-6 were used to assess *in vivo* anticancer effect FMMPG.

***In vivo* antitumor evaluation**

Animal experimental procedures were executed in accordance with the Guidelines for Care and Use of Laboratory Animals of the Drug Safety Evaluation Center of Harbin Medical University (No. SYDW 2019-82). Typically, the tumor xenograft was established in the left axilla of each female mouse (15-20 g). After the tumor size increased approximately 6-8 mm, the Kunming female mice were randomly fell into six groups (each group with five mice) followed by injection with U14 cells to left axilla and dealt with different conditions as followed: (1) Control, (2) Control + Laser, (3) FMMP; (4) FMMP + Laser (0.6 W cm^{-2}, 10 min), (5) FMMPG; (6) FMMPG + Laser (0.6 W cm^{-2}, 10 min), respectively. The tumor sizes and weights of the mice were measured once two days. The tumor volume (mm^3) of mice was calculated by the formula $V = lw^2/2$, in which l and w respectively are the length and width of the tumor. The injection dose for FMMPG in this assay is 100 μL (200 μg mL^{-1}).

Biodistribution

The mice were injected intravenously with FMMPG or FMMSNs, then were euthanized at time points of 0 h, 6 h, 12 h and 24 h. The collected major tissues (heart, liver, spleen, lung, kidney, and tumor) were dissolved in aqua regia. To obtain clear solutions, the mixture was heated to 70 °C, maintained for 5 min, and centrifuged for further ICP-OES analysis.

Metabolism study

The urine of U14-tumor-bearing mice were collected at different time points after FMMPG administration (0, 6, 12 and 24 h), then treated with aqua regia for dissolution. The contents of Fe in urine were measured by ICP-OES.

Blood hematology and biochemistry analysis

Ten healthy Kunming female mice were divided into two groups (n = 5 per group). One was used as a control group, and the other group was injected with 50 μL FMMPG solution (500 μg mL^{-1}). After 14 days, the blood samples were obtained by extracting eyeball blood to test the blood routines and serum biochemistry indicators.

Statistical analysis

All experiments were performed at least three times, and the results are expressed as mean ± standard deviation (S.D.). The specific statistical sample size for each experiment is shown in the Figure legend. For two group comparisons, two-tailed Student's t-tests were used. For multiple comparisons, one-way analysis of variance (ANOVA) with Tukey's post-hoc test was used. ns means no significance. *$p < 0.05$ was considered statistically significant, whereas **$p < 0.01$ and ***$p < 0.001$ were considered highly and extremely significant. The Origin 2017 software was used for graph plotting.

Table S1. The contents of Fe and Mn on FMMSNs tested by ICP-OES.

Elements	**Fe**	**Mn**
Wt (%)	14.49	3.21

Table S2. EXAFS fitting parameters at the Fe/Mn *K*-edge for various samples.

Sample	Shell	*CN*[a]	*R*(Å)[b]	σ^2(Å^2)[c]	ΔE_0(eV)[d]	*R* factor
			Fe K-edge (S_0^2=0.787)			
Fe foil	Fe-Fe	8*	2.4733±0.003	0.0047±0.0003	6.9±0.6	0.0016
	Fe-Fe	6*	2.849±0.004	0.0061±0.0006		
FeO	Fe-O	6.0±0.2	2.217±0.014	0.0163±0.0141	9.5±3.3	0.0026
	Fe-Fe	11.5±0.4	3.081±0.015	0.0185±0.0146	5.6±2.1	
Fe_2O_3	Fe-O	6.0±0.6	1.963±0.025	0.0132±0.0035	-4.2±3.8	0.0092
	Fe-Fe	5.3±0.3	2.976±0.015			
	Fe-Fe	5.3±0.3	3.469±0.014	0.0079±0.0018	3.3±2.5	
	Fe-Fe	3.9±0.1	3.723±0.026			
FMMPG	Fe-O	3.4±0.1	1.947±0.027	0.0093±0.0047	-0.7±3.8	0.0118
	Fe-Mn	2.2±0.5	3.132±0.019	0.0107±0.0020	7.7±8.6	
			Mn K-edge (S_0^2=0.752)			
Mn foil	Mn-Mn	12*	2.682±0.015	0.0071±0.0018	6.9±2.6	0.0050
MnO	Mn-O	6.0±0.6	2.204±0.008	0.0092±0.0009	0.1±1.1	0.0075
	Mn-Mn	11.2±0.7	3.131±0.018	0.0074±0.0024	2.9±2.6	
MnO_2	Mn-O	6.1±0.5	1.898±0.005	0.0034±0.0005	1.6±1.2	0.0094
	Mn-Mn	3.2±0.4	2.861±0.009	0.0040±0.0007	-2.7±1.9	
	Mn-Mn	3.5±0.5	3.438±0.012		-0.2±2.3	
Mn_2O_3	Mn-O	6.0±0.8	1.896±0.010	0.0049±0.0011	-1.3±2.2	0.0181
	Mn-Mn	9.3±0.4	3.133±0.009	0.0075±0.0010	5.9±0.4	
FMMPG	Mn-O	2.4±0.4	1.883±0.007	0.0019±0.0017	-1.8±1.0	0.0058
	Mn-Fe	2.4±0.4	3.135±0.022	0.0078±0.0032	-7.3±3.0	

[a]*C.N*, coordination number; [b]*R*, the distance to the neighboring atom; [c]σ^2, the Mean Square Relative Displacement (MSRD); [d]ΔE_0, inner potential correction; *R* factor indicates the goodness of the fit. S_0^2 was fixed to 0.787, 0.752 and 0.891, according to the experimental EXAFS fit of Fe foil, Mn foil by fixing *CN* as the known crystallographic value. * This value was fixed during EXAFS fitting, based on the known structure of Fe, Mn. Fitting range: 3.0 ≤

k (/Å) ≤ 14.1 and 1.0 ≤ R (Å) ≤ 3.0 (Fe foil); 3.0 ≤ k (/Å) ≤ 11.2 and 1.0 ≤ R (Å) ≤ 3.0 (FeO); 3.0 ≤ k (/Å) ≤ 12.4 and 1.0 ≤ R (Å) ≤ 4.0 (Fe2O3); 1.0 ≤ k (/Å) ≤ 10.00 and 1.0 ≤ R (Å) ≤ 3.0 (684-Fe-1); 3.0 ≤ k (/Å) ≤ 13.00 and 1.8 ≤ R (Å) ≤ 3.0 (Mn foil); 3.0 ≤ k (/Å) ≤ 12.38 and 1.0 ≤ R (Å) ≤ 3.5 (MnO); 3.0 ≤ k (/Å) ≤ 14.00 and 1.0 ≤ R (Å) ≤ 4.0 (MnO2);3.0 ≤ k (/Å) ≤ 13.90 and 1.0 ≤ R (Å) ≤ 3.5 (Mn2O3); 1.0 ≤ k (/Å) ≤ 10.00 and 1.0 ≤ R (Å) ≤ 3.5 (684-Mn-1); 3.0 ≤ k (/Å) ≤ 14.0 and 1.0 ≤ R (Å) ≤ 3.5A reasonable range of EXAFS fitting parameters: 0.700 < S_0^2 < 1.000; CN > 0; σ^2 > 0 Å^2; $|\Delta E_0|$ < 10 eV; R factor < 0.02.

Table S3. The atomic ratio between Fe and Mn on FMMPG.

Experimental	4:1	2:1	1:1
Detected (ICP)	10:1	5:1	2:1

Table S4. Blood biochemical assay and hematology analysis of tumor-bearing mice in control (saline injection) and treatment group (FMMPG injection plus 650 nm irradiation).

Tests	Units	Control (mean ± sd)	Treatment (mean ± sd)
Biochemistry			
AST	U/L	22.3±5.8	25.6±2.4
ALT	U/L	23.2±4.8	32.4±3.2
ALP	U/L	138.8±3.2	130.2±5.2
TP	g/L	57.0±5.2	56.8±2.3
Hematological			
WBC	$\times 10^9$/L	6.8±1.6	7.2±1.8
NE	$\times 10^9$/L	5.4±2.3	6.3±2.6
LY	$\times 10^9$/L	1.4±0.4	1.6±0.3
RBC	$\times 10^{12}$/L	5.7±1.2	6.5±1.6
HGB	g/L	143.5±13.4	141.8±20.3
MCV	fL	92.5±3.2	94.70±2.14
MCH	pg	32.2±3.5	29.40±1.2
MCHC	g/L	365.8±4.2	361.0±4.7
RDW	%	15.40±3.4	14.50±1.85
PLT	$\times 10^9$/L	220.3±63.5	240.3±32.7

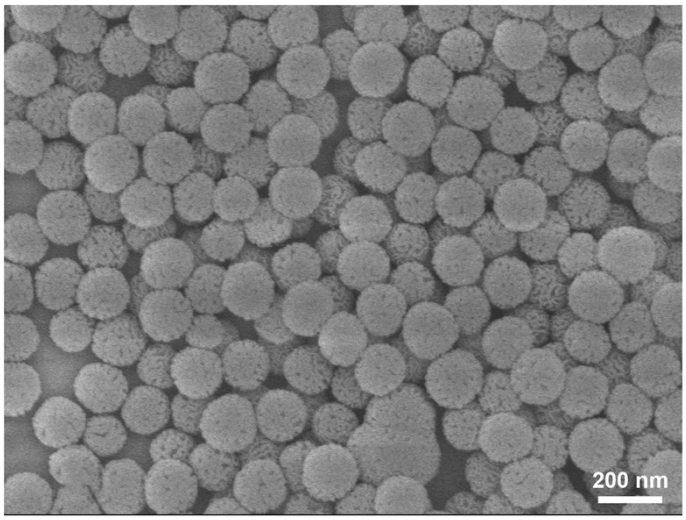

Fig. S1. SEM image of MSNs.

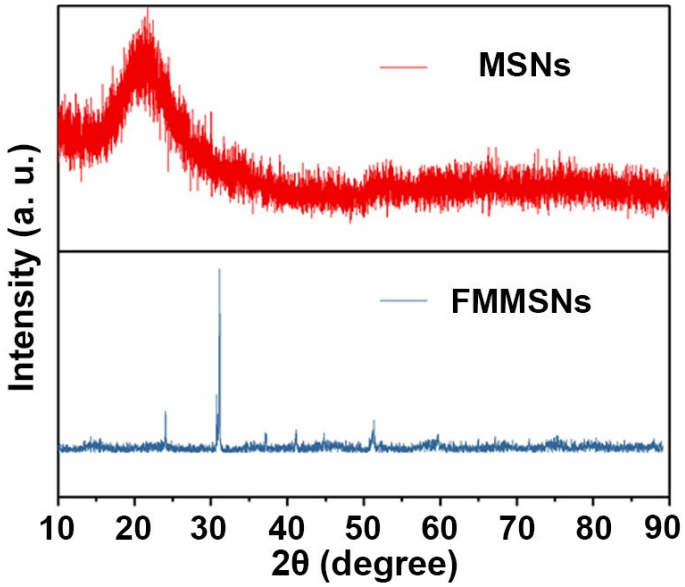

Fig. S2. XRD pattern of MSNs and FMMSNs.

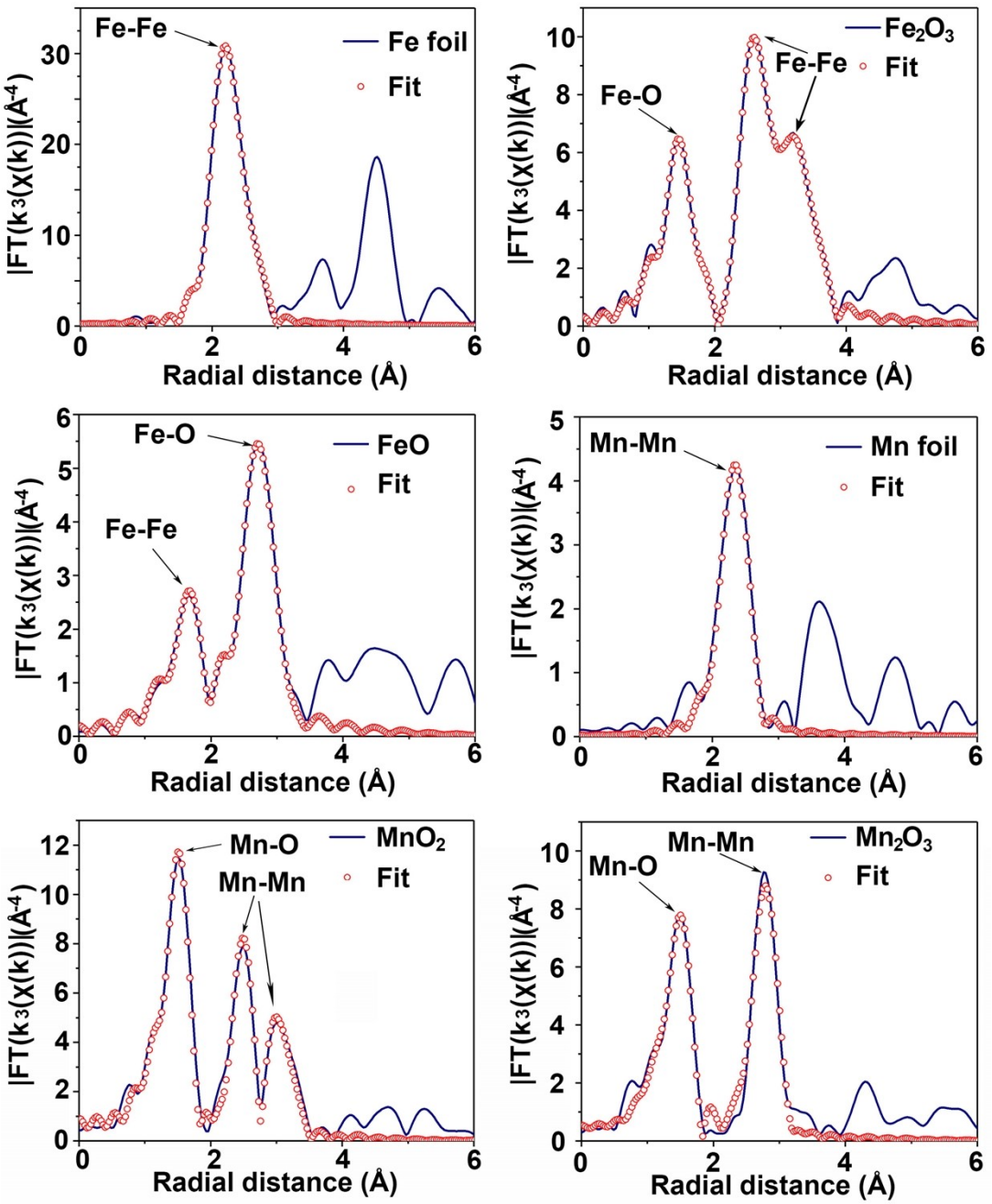

Fig. S3. FT k^3-weighted EXAFS fitting curves at *R*-space of Fe foil, Fe_2O_3, FeO, Mn foil, MnO_2 and Mn_2O_3.

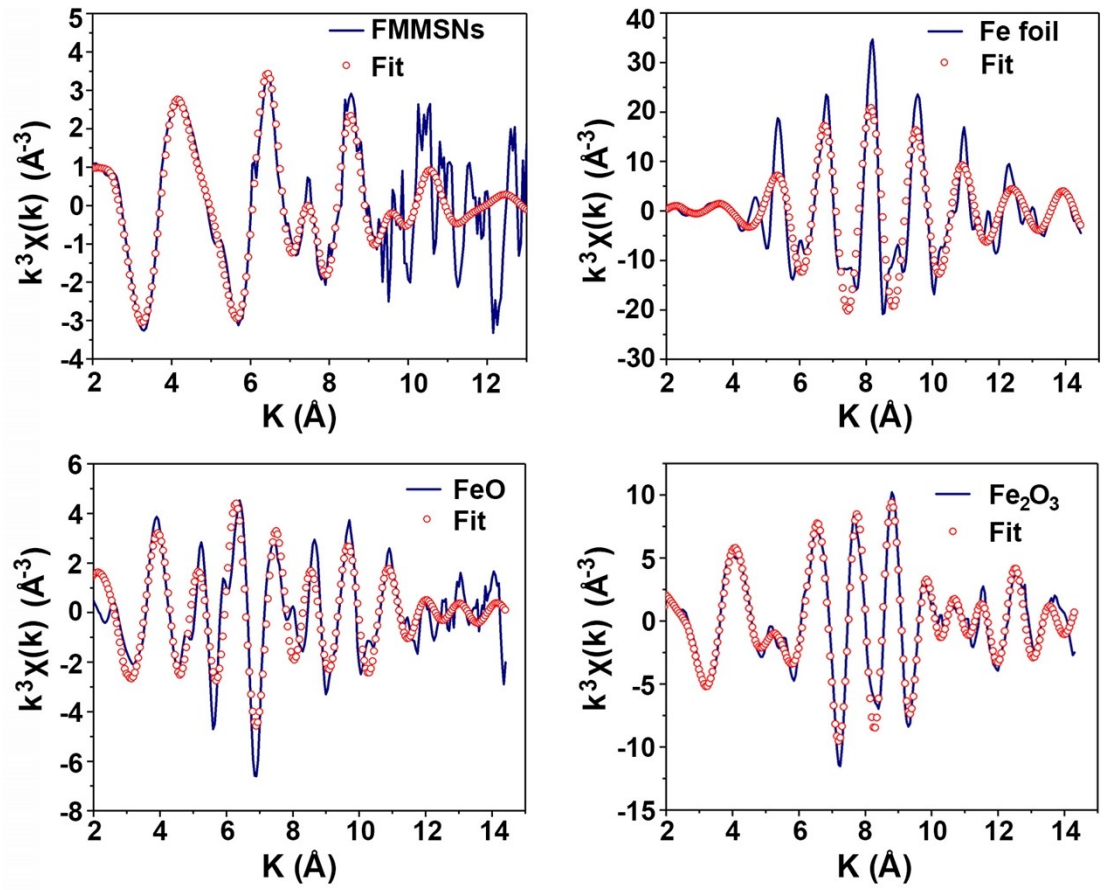

Fig. S4. $K^3\chi(k)$ space spectra fitting curves of FMMSNs, Fe foil, FeO and Fe_2O_3.

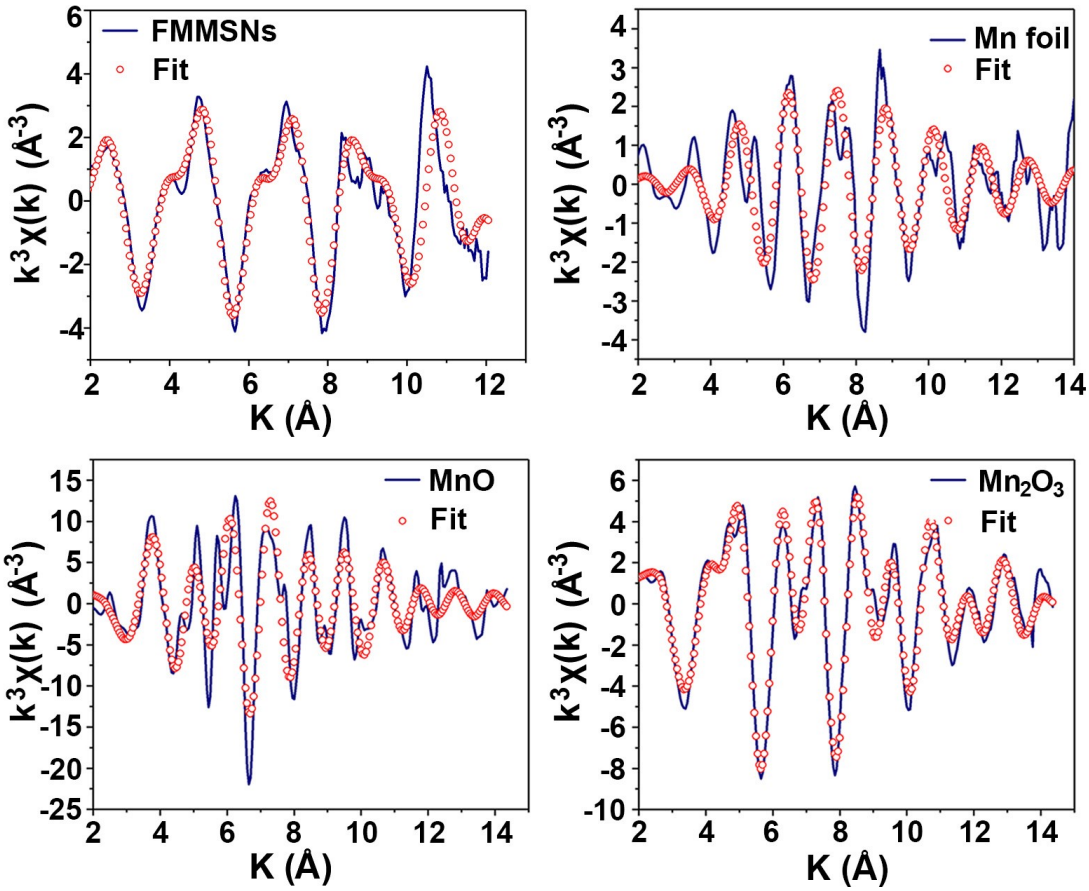

Fig. S5. $K^3\chi(k)$ space spectra fitting curves of FMMSNs, Mn foil, MnO and Mn_2O_3.

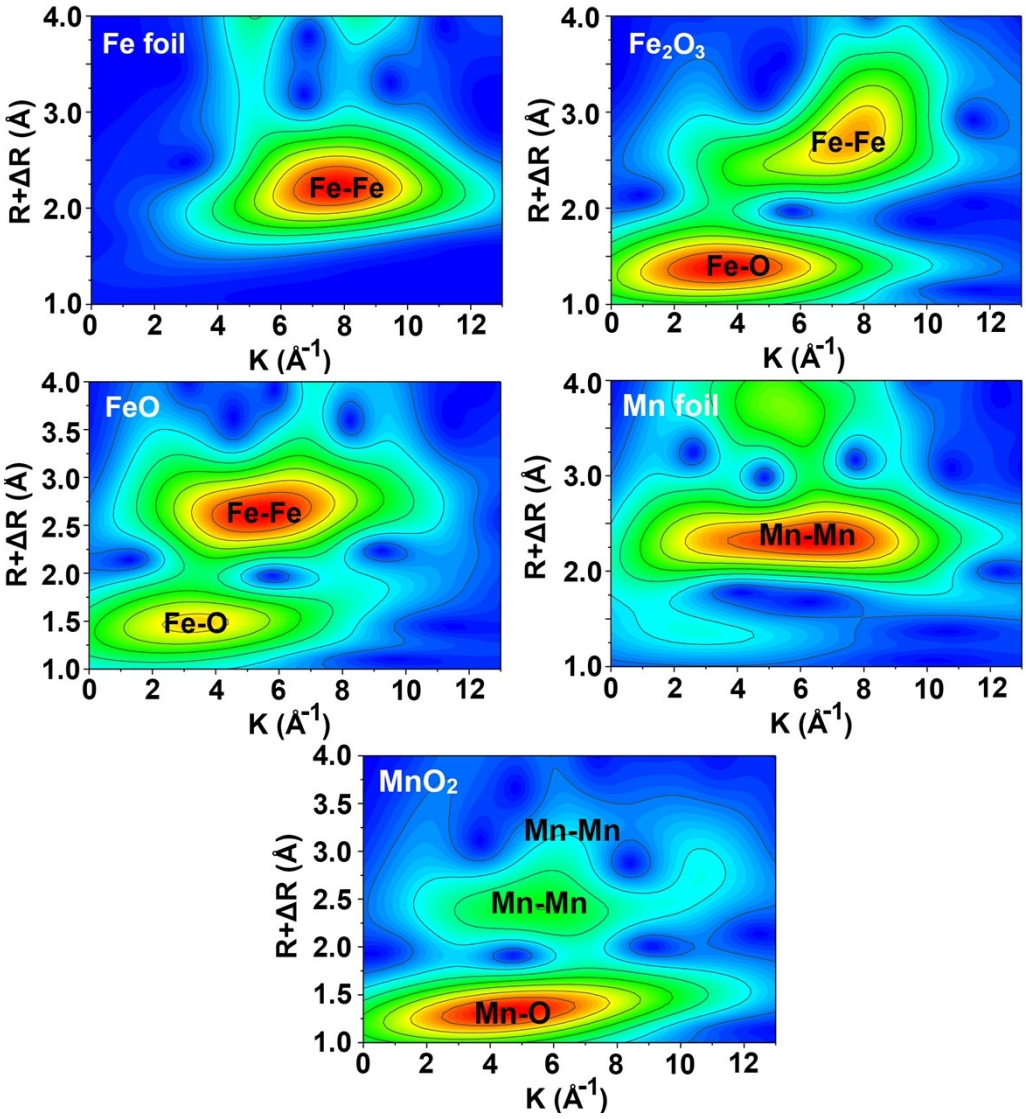

Fig. S6. WT-EXAFS contour maps of Fe foil, Fe_2O_3, FeO, Mn foil, and MnO_2.

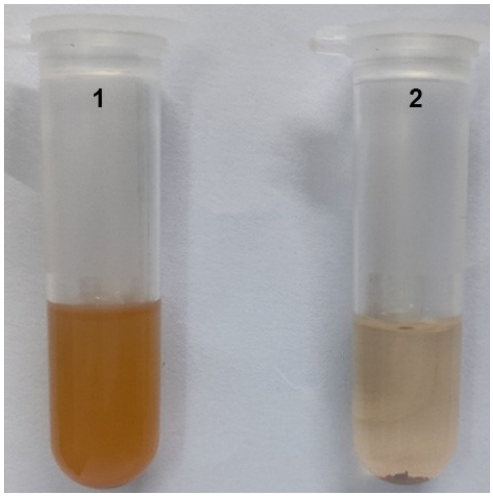

Fig. S7. The photograph of FMMP (1) and FMMSNs (2) at PBS of pH 6.5 and GSH 10 mM condition.

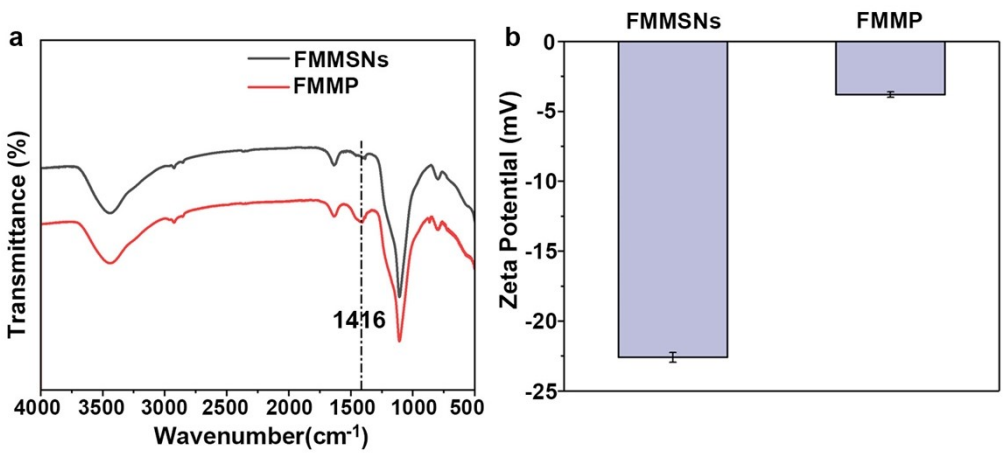

Fig. S8. FT-IR spectra of FMMSNs and FMMP samples (a). Surface ζ potential of FMMSNs and FMMP samples (b).

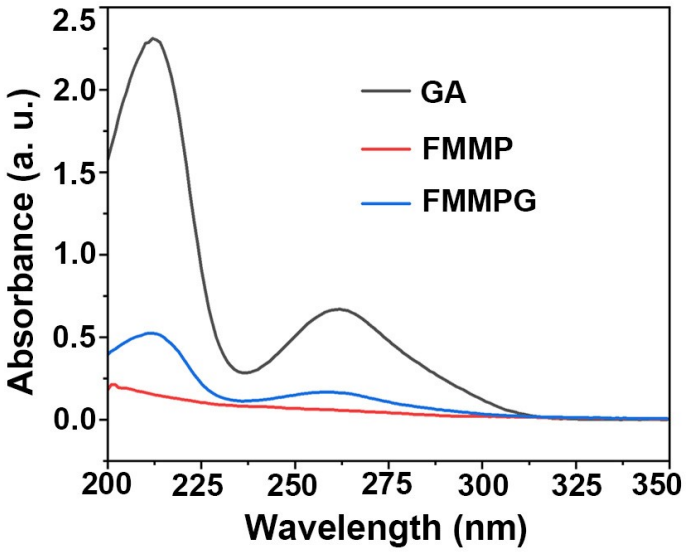

Fig. S9. UV-vis absorption spectra of GA, FMMP and FMMPG.

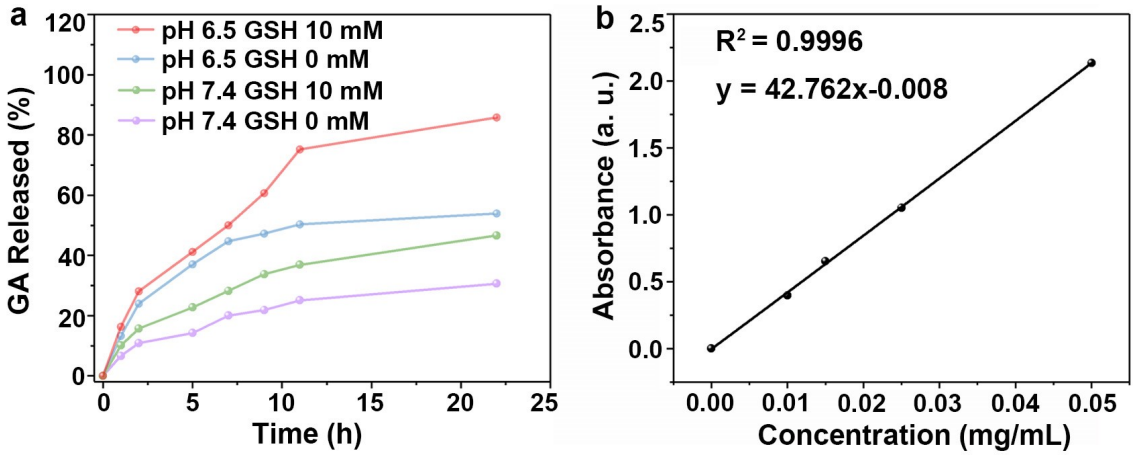

Fig. S10. Cumulative drug release behavior of GA with different conditions (a). The linear equation of the relationship between the concentration of GA solution and the absorbance at wavelength 265 nm (b).

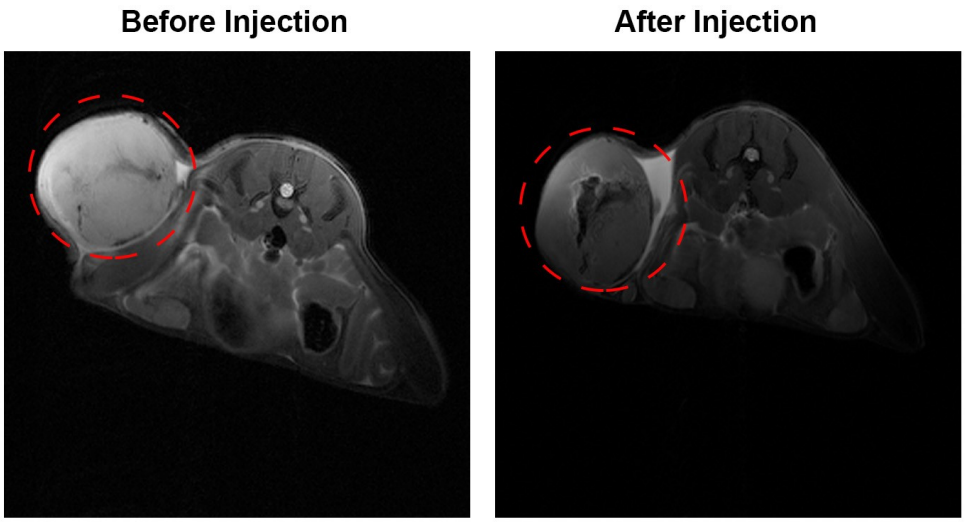

Fig. S11. *In vivo* T_2-weighted MR images of tumor-bearing mice before and after injection of FMMSNs.

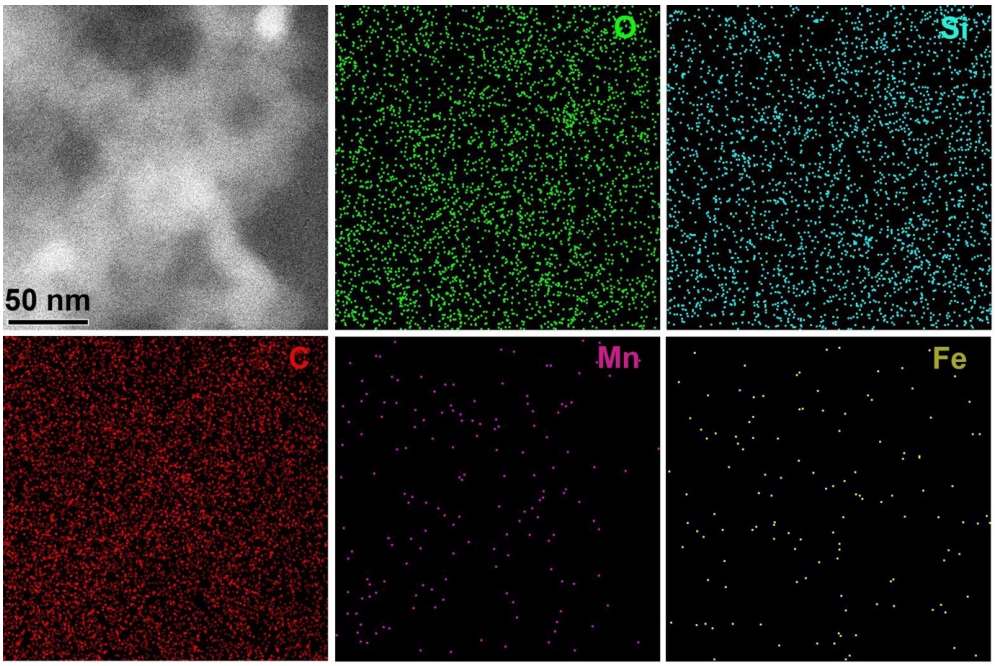

Fig. S12. EDS mapping images of the M-GA.

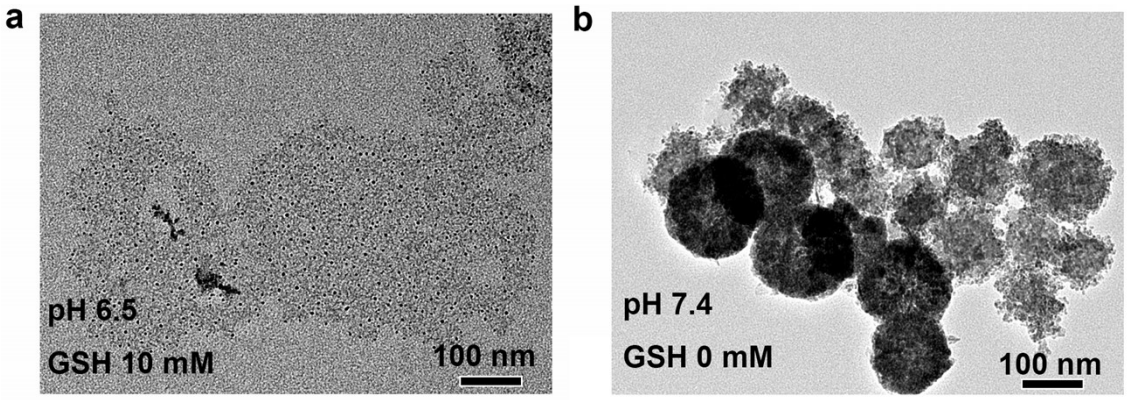

Fig. S13. TEM images of FMMPG (1 mg mL^{-1}) treated at PBS solutions (pH 6.5 10 mM GSH) (a) and (pH 7.4) (b) for 24 h.

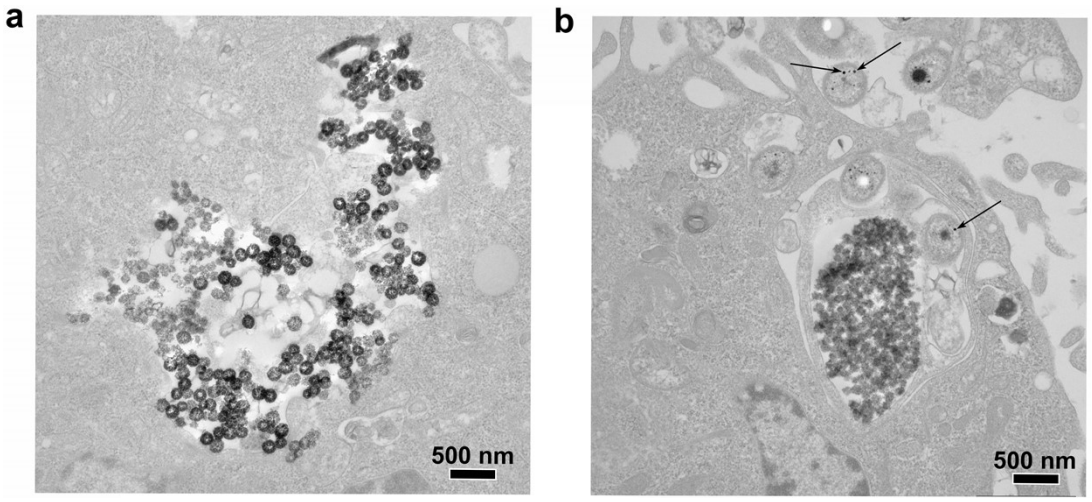

Fig. S14. Bio-TEM images of HeLa cells incubated with FMMPG nanoparticles for 1 h (a), 18 h (b).

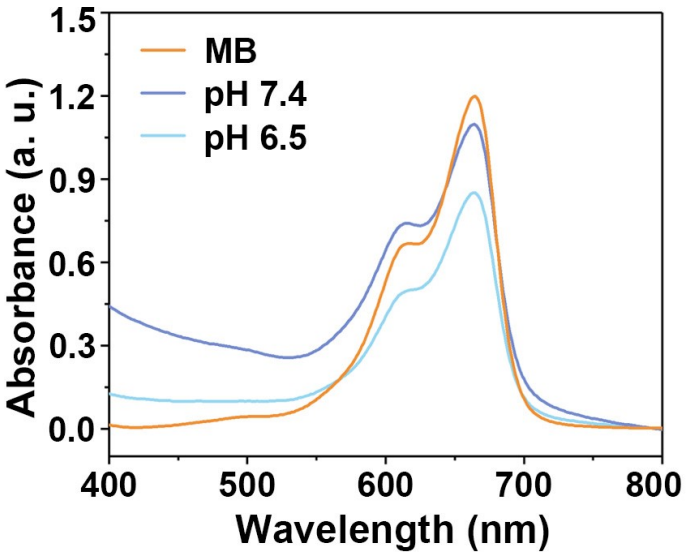

Fig. S15. MB degradation by •OH generated by treating with FMMPG (200 μg mL^{-1}) under different pH.

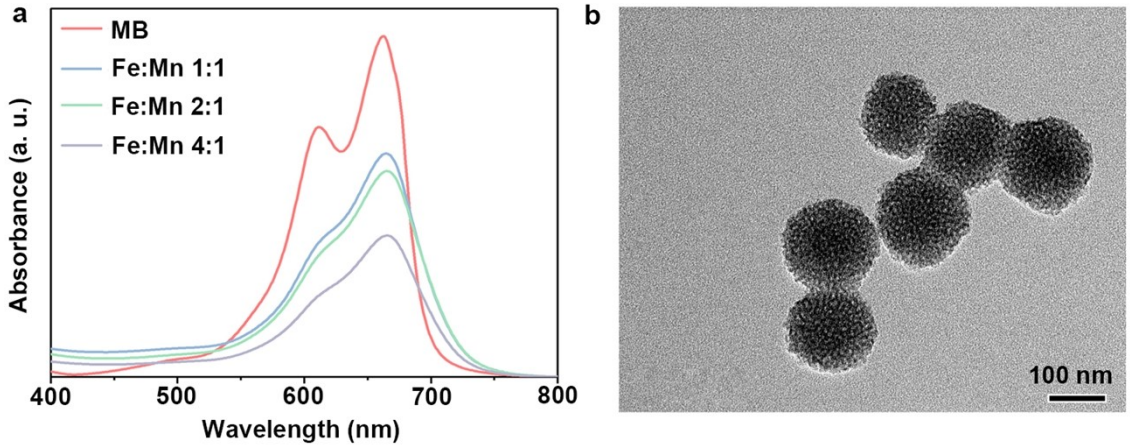

Fig. S16. MB degradation by FMMPG with different molar ratio of Fe and Mn in the condition of pH 6.5 plus H_2O_2 (10 mM) and GSH (10 mM) (a). TEM image of FMMSNs with the molar ratio of Fe and Mn at 4:1 (b).

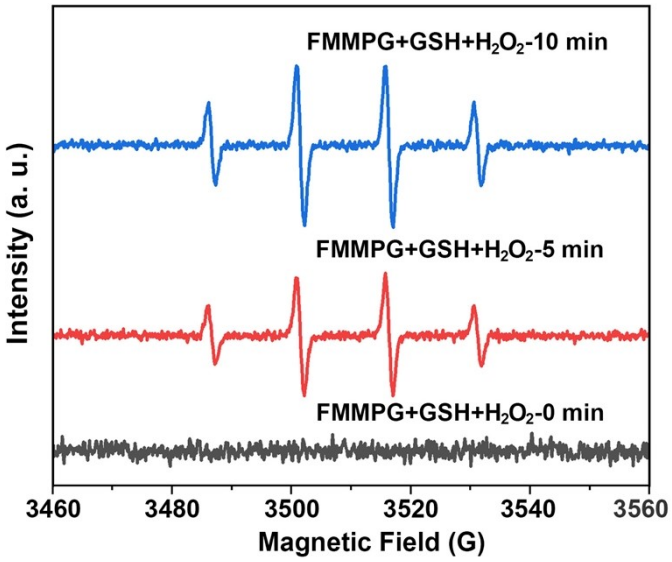

Fig. S17. ESR spectra of •OH detection for FMMPG in the condition of pH 6.5 plus H_2O_2 (10 mM) and GSH (10 mM).

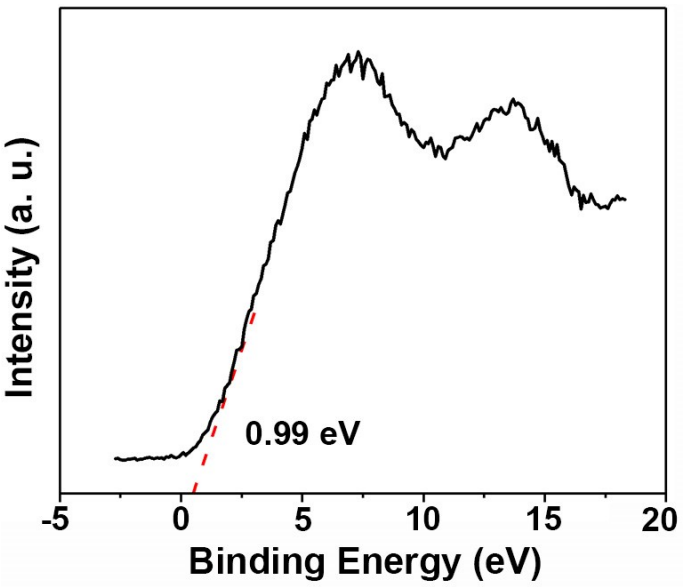

Fig. S18 . The VB-XPS spectrum of FMMSNs.

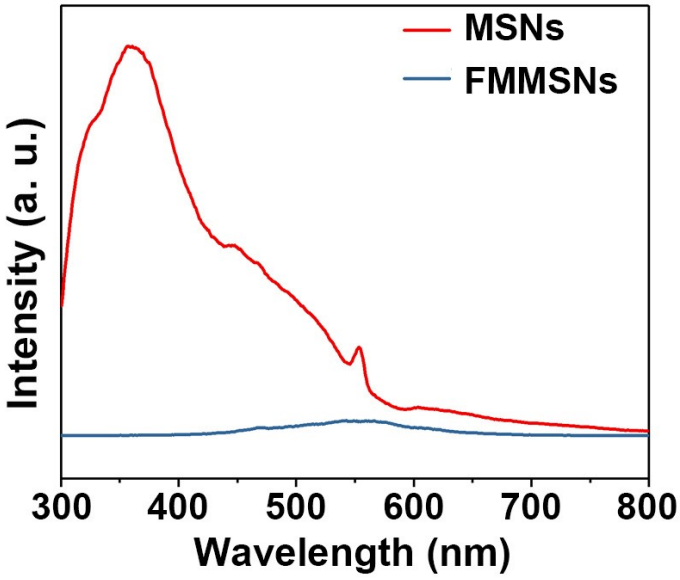

Fig. S19. Photoluminescence spectra of MSNs and FMMSNs.

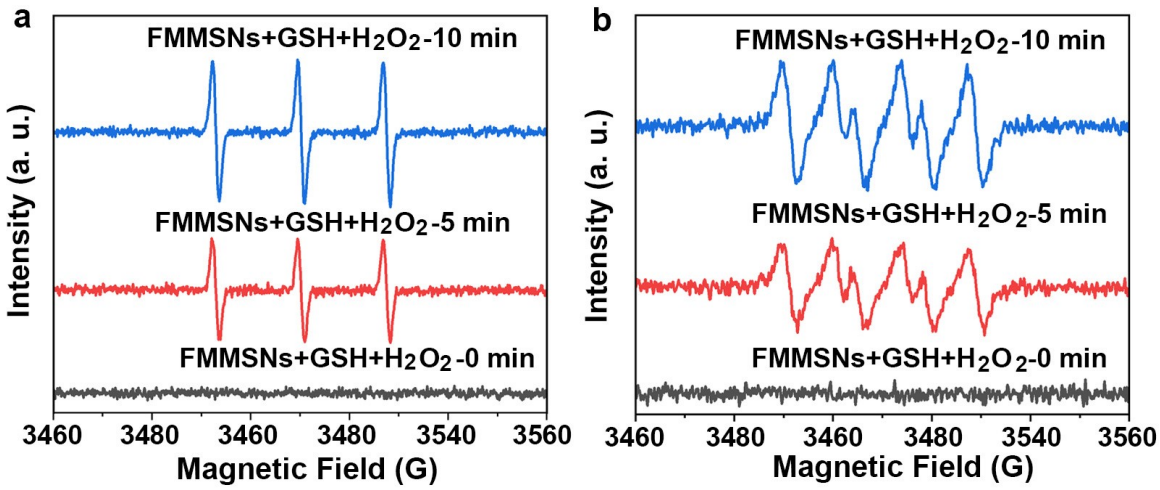

Fig. S20. ESR spectra of $^1O_2$ (a) and $\bullet O_2^-$ (b) generation in the condition of pH 6.5 plus H_2O_2 (10 mM) and GSH (10 mM).

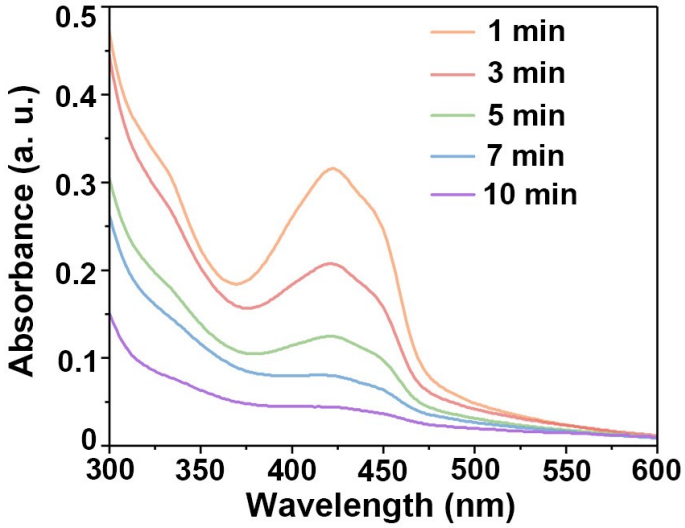

Fig. S21. Time-dependent degradation of DPBF caused by $^1O_2$.

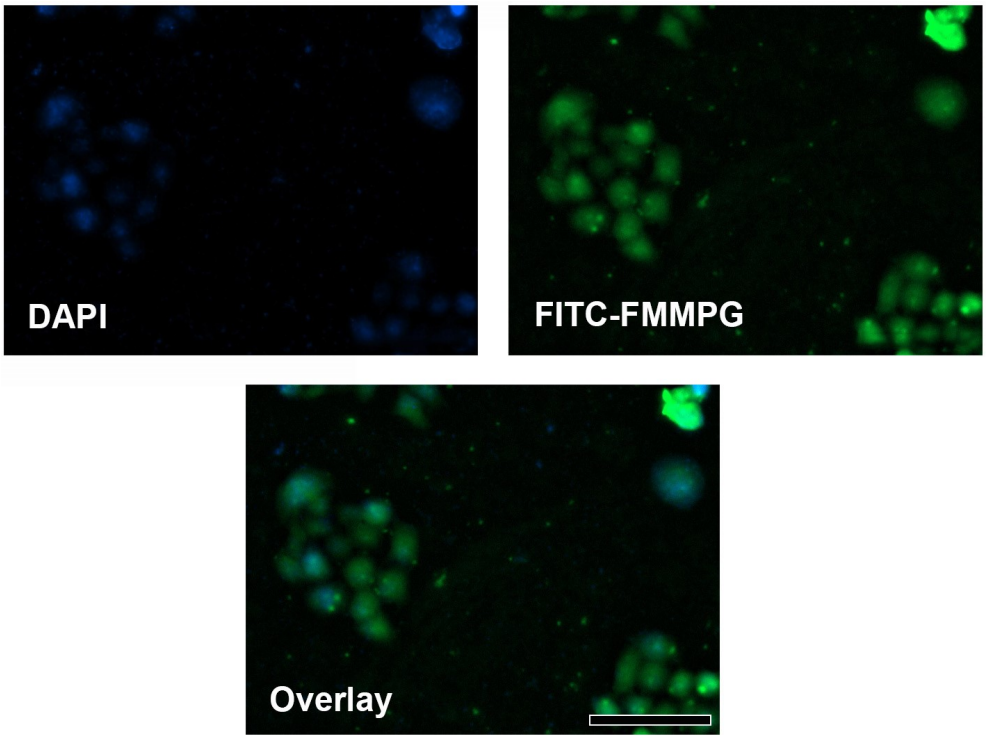

Fig. S22. CLSM images of HeLa cells after treatment with FITC-FMMPG for 1 h. Scale bar: 100 μm.

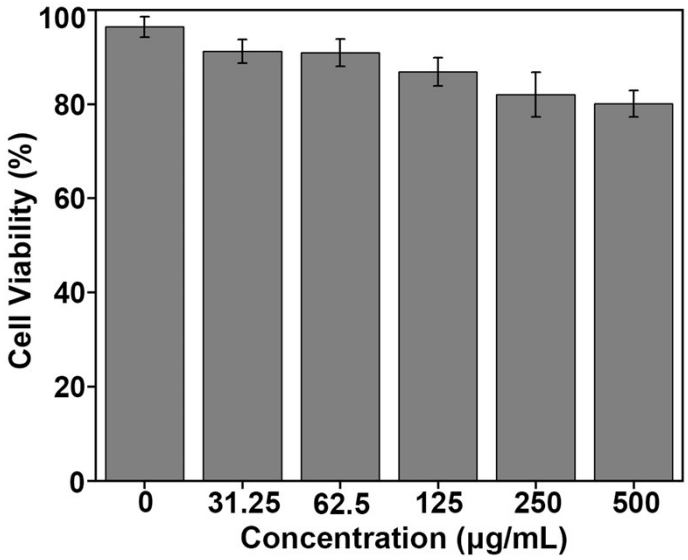

Fig. S23. Viabilities of L929 cells treated with FMMPG.

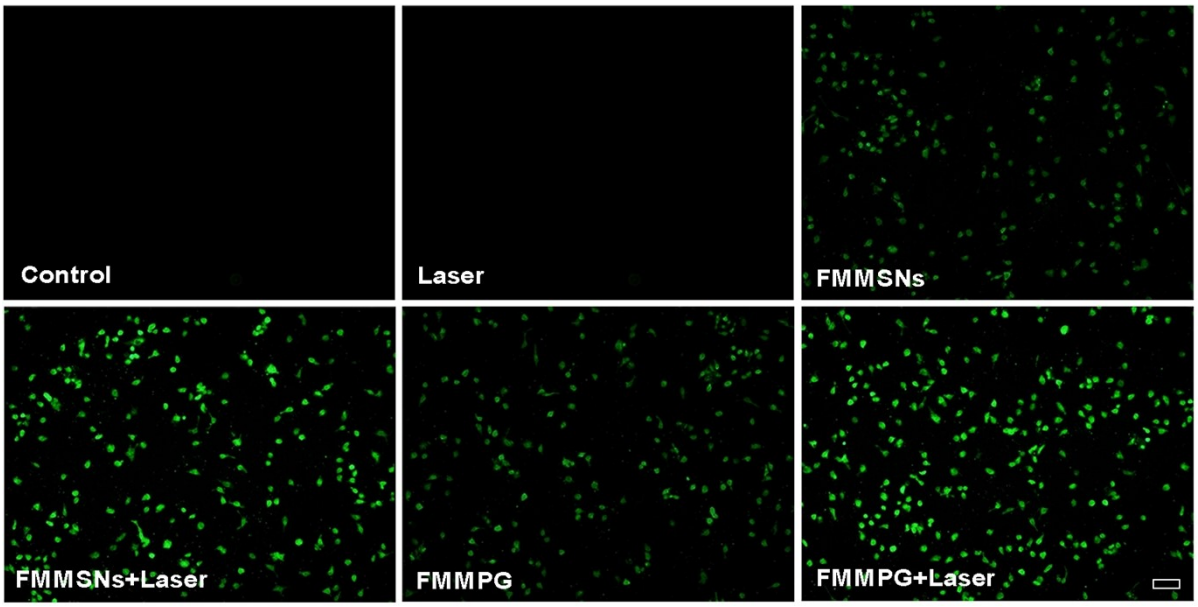

Fig. S24. Production of $^1O_2$ at the cellular level detected by SOSG probe. Scale bar: 50 μm.

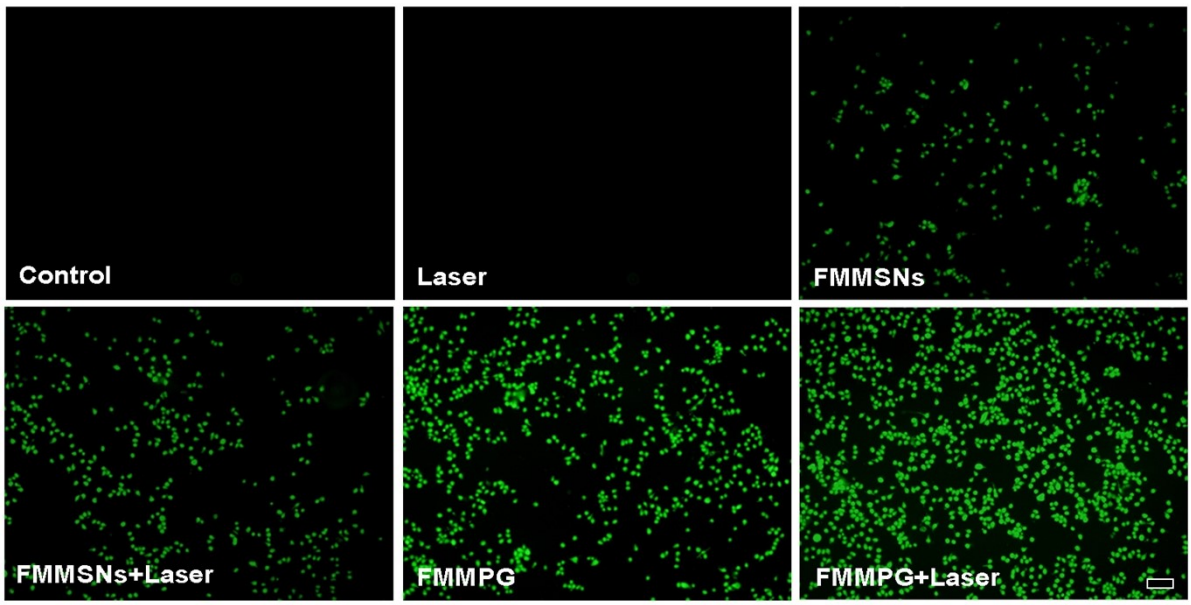

Fig. S25. Production of •OH at the cellular level detected by HPF probe. Scale bar: 50 μm.

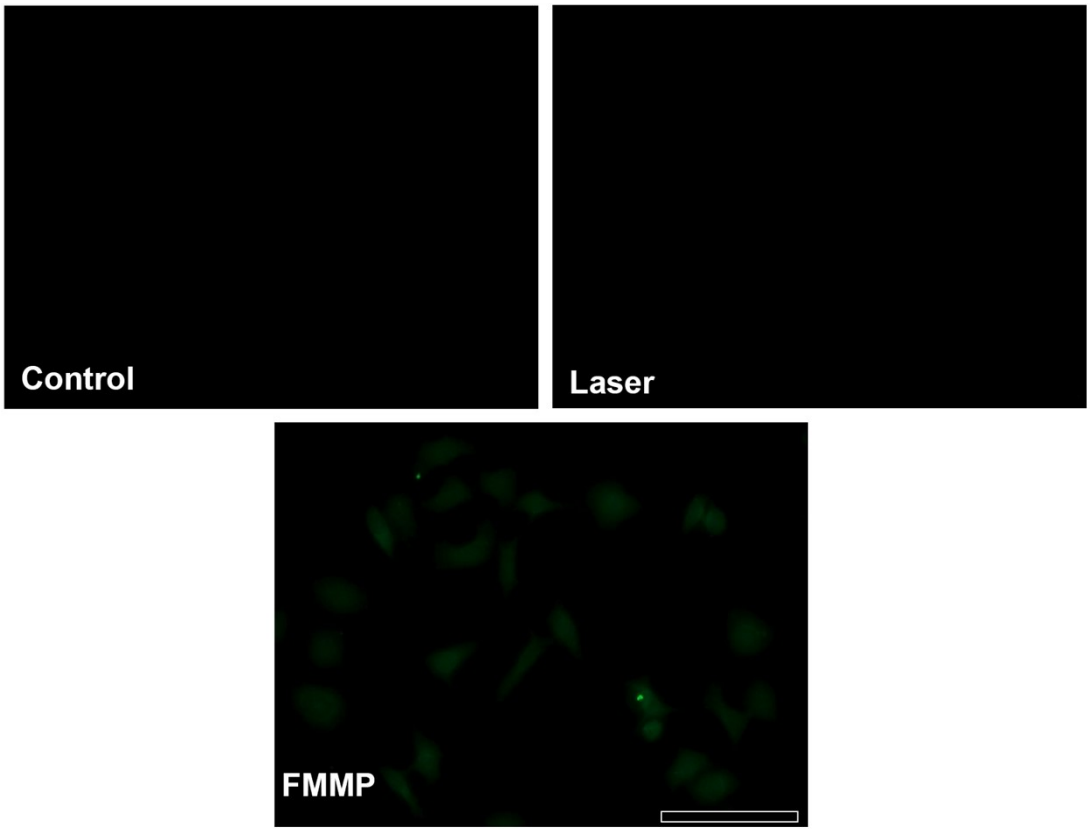

Fig. S26. Intracellular ROS detection using DCFH-DA probe in the Control, Laser and FMMP groups. Scale bar: 100 μm.

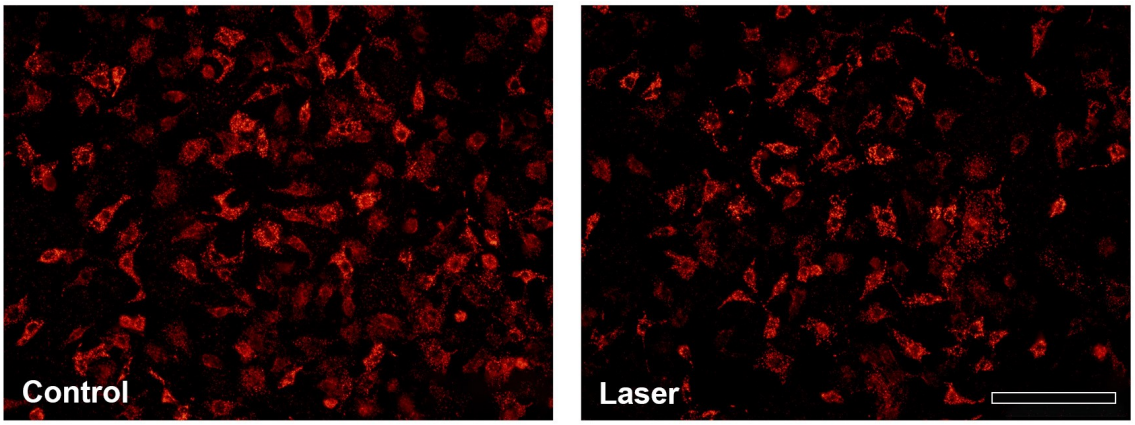

Fig. S27. CLSM images of HeLa cells stained by JC-1 after different treatments of Control and Laser. Scale bar: 100 μm.

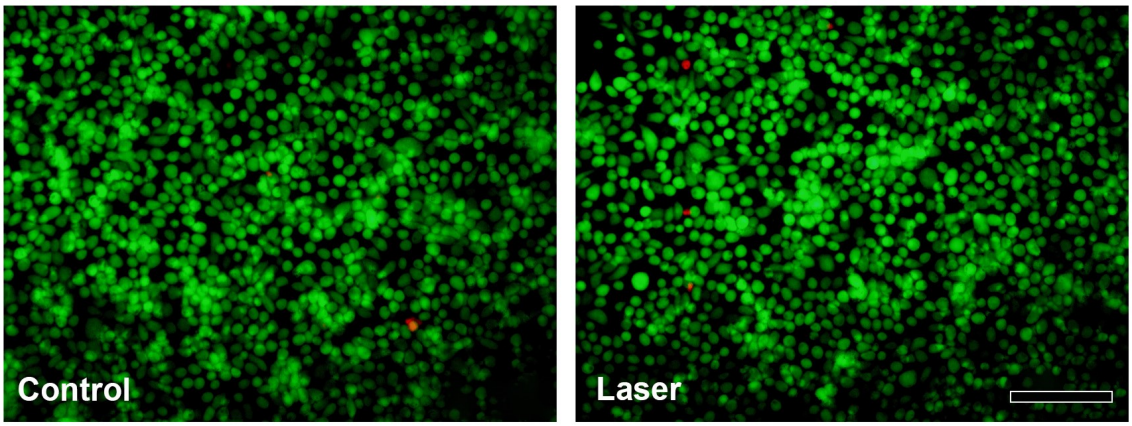

Fig. S28. CLSM images dyed with AM and PI of HeLa cells in the Control and Laser groups.

Scale bar: 100 μm.

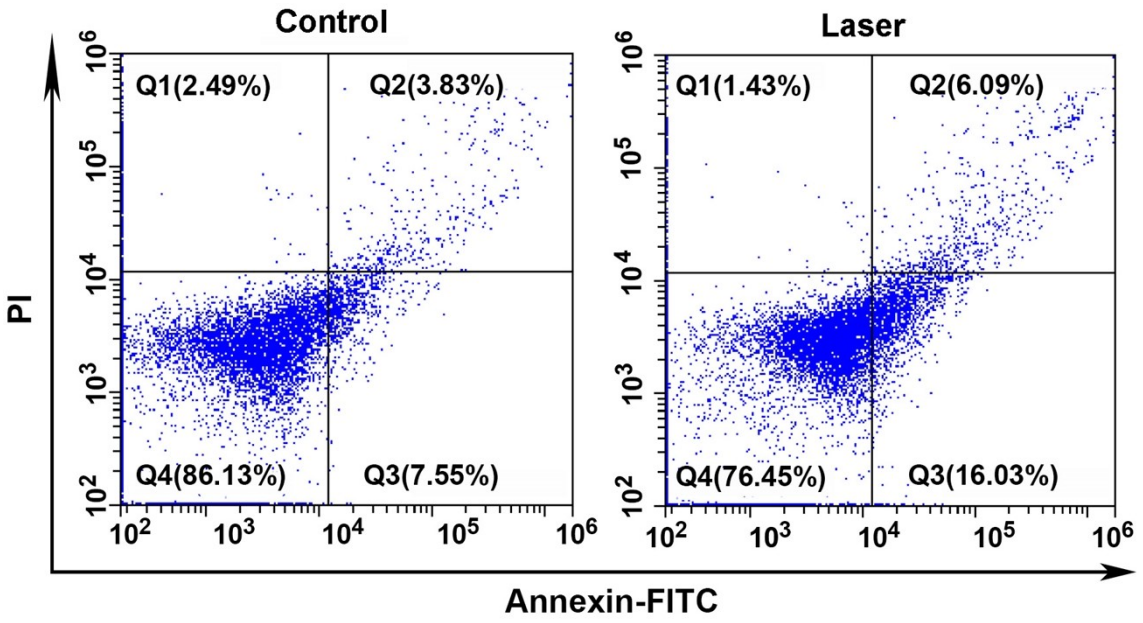

Fig. S29. Apoptosis of HeLa cells detected by flow-cytometry in the groups of Control and Laser.

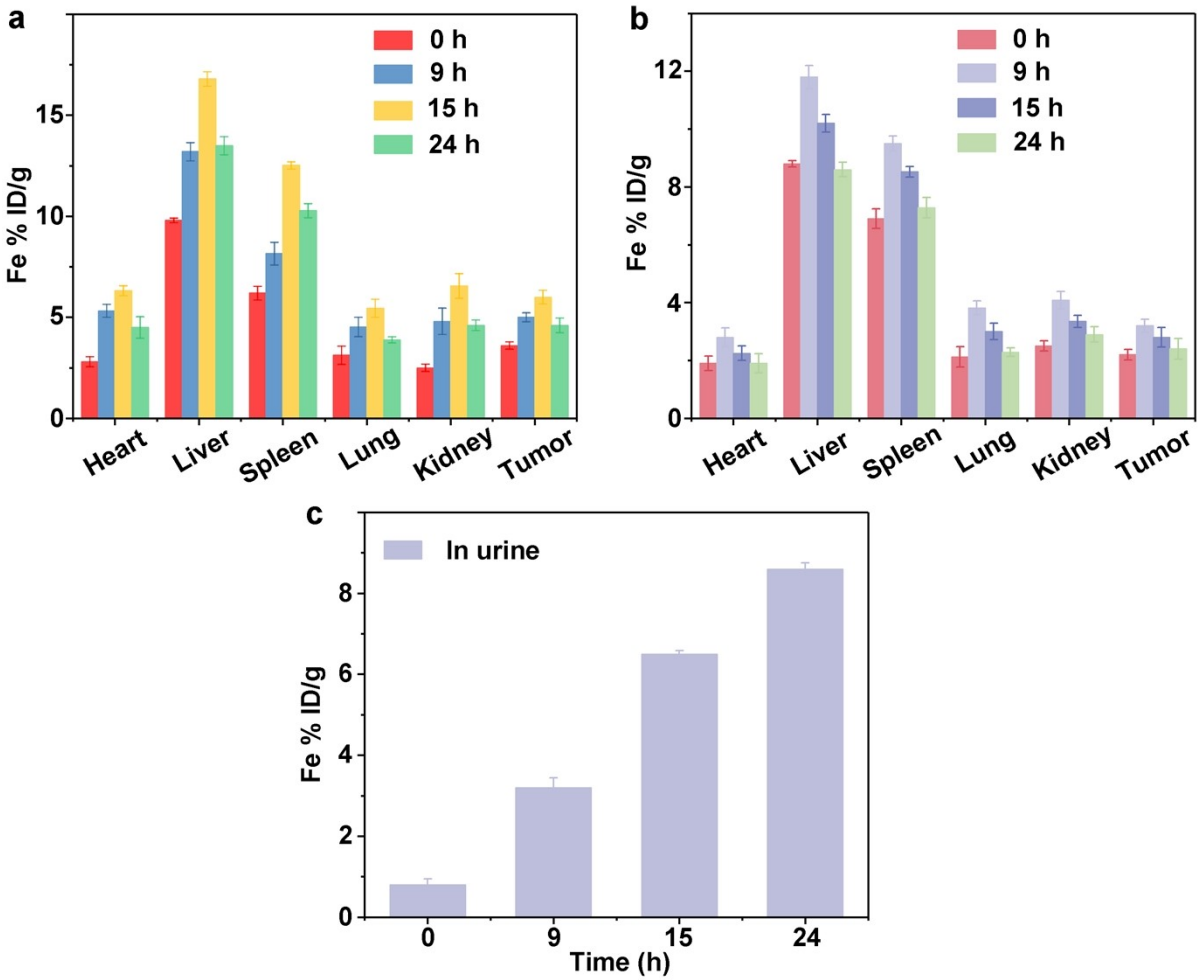

Fig. S30. Distribution of Fe element in main organs (heart, liver, spleen, lung, and kidney) and tumor of mice at varied time points after FMMPG (a) and FMMSNs (b) administration. Time-dependent Fe excretions from tumor-bearing mice after FMMPG administration (c).

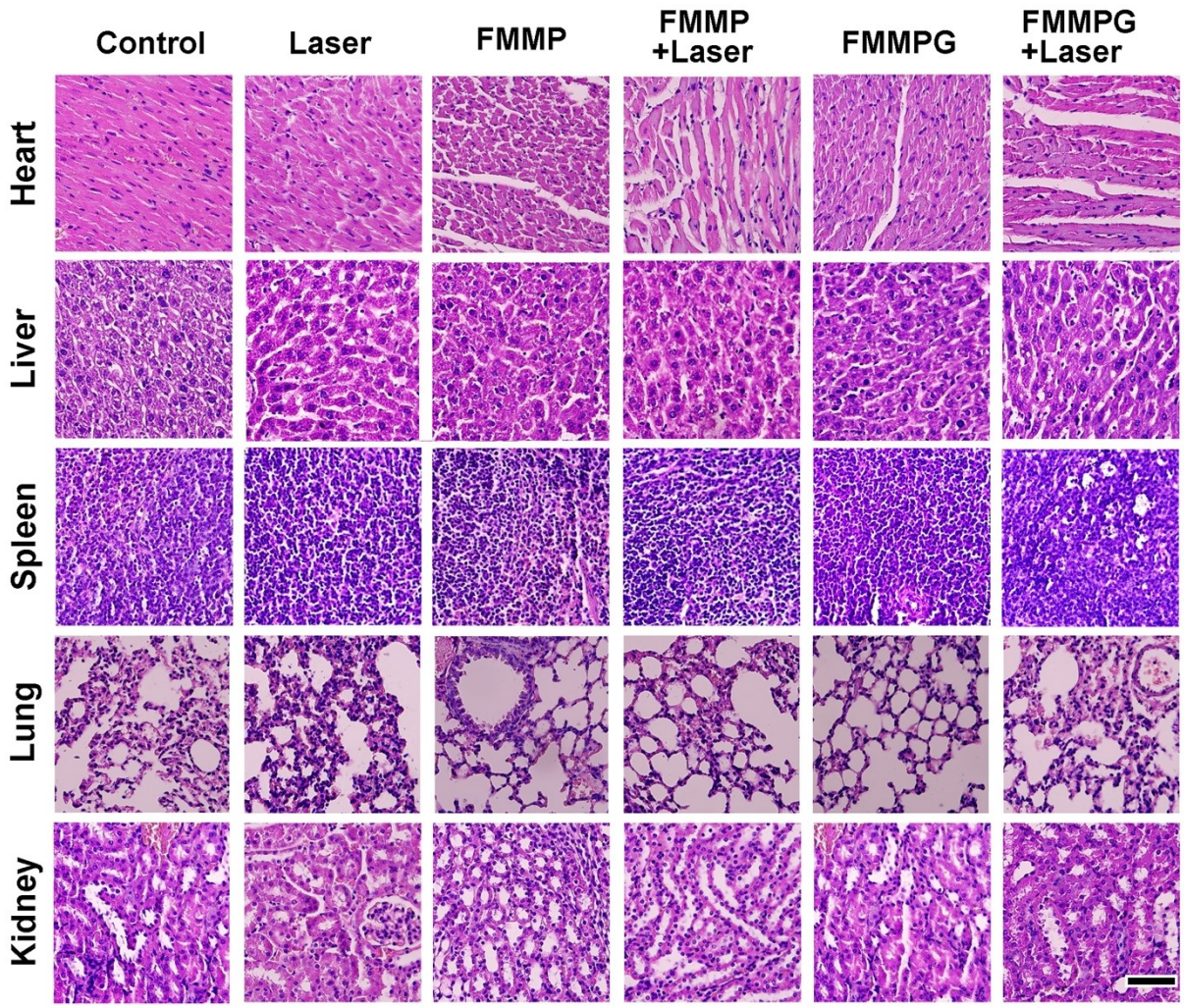

Fig. S31. H&E-stained tissue sections of major organs (including heart, liver, spleen, lung, and kidney) from tumor-bearing mice receiving various treatments. Scale bar: 100 μm.